Angular spectrum of diffracted wave fields with apochromatic correction

Carlos J. Zapata-Rodríguez,[1] María T. Caballero,[2] and Juan J. Miret[2]

[1]*Departamento de Óptica, Universidad de Valencia, 46100 Burjassot, Spain*
[2]*Departamento de Óptica, Universidad de Alicante, P.O. Box 99, Alicante, Spain*
**Corresponding author: carlos.zapata@uv.es*

Received March 5, 2008; revised June 17, 2008; accepted June 28, 2008;
posted July 9, 2008 (Doc. ID 93491); published July 30, 2008

We report on compensation of diffraction-induced angular dispersion of ultrashort pulses up to a second order. A strategy for chromatic correction profits from high dispersion of kinoform-type zone plates. Ultraflat dispersion curves rely on a saddle point that may be tuned at a prescribed wavelength. Validity of our approach may reach the few-cycles regime. © 2008 Optical Society of America

OCIS codes: 050.1970, 320.0320, 220.4830.

Diffraction gratings are optical elements with the ability of separate time spectral components of broadband radiation, thus widely used in wavelength-demultiplexing and spectroscopy. The physical mechanism of this phenomenon relies on the space-time coupling involving diffraction. In particular, excitation of a given spatial frequency causes the onset of a tilted plane wave in which the propagation direction is chromatically dispersed [1,2]. In the angular-spectrum representation, diffraction leads to variant spectra at different temporal frequencies. Diffraction-induced angular dispersion (DIAD) results in a major inconvenience in many other applications. For instance, a diffractive optical element (DOE) designed to tailor the shape of a monochromatic field would bring about substantial deviations of the prescribed waveform if it is applied over ultrabroadband laser beams [3].

Some proposals are found in the literature concerning compensation of DIAD employing highly dispersive prisms and gratings [4,5]. In particular, kinoform-type zone plates (ZPs) are energetically efficient solutions leading to chromatic dispersion isotropically around the optic axis. Previously, we developed ZP-based compensating achromatic setups demonstrating modest behavior in ultrabroadband regimes [6,7]. In this Letter we propose a novel arrangement consisting of an appropriate combination of ZP doublets capable of transforming a diffracted wave field to exhibit zero DIAD of its angular-spectrum components at a given wavelength, providing an apochromatic response.

The chromatic operation of a ZP doublet is as follows. The pair of ZPs, namely ZP_1 and ZP_2 in Fig. 1, are separated a distance $d \geqslant 0$. If the focal distance of ZP_n is Z_n ($n=\{1,2\}$) for a wavelength λ_0, it changes following an inverse law upon the wavelength as $f_n = Z_n\lambda_0/\lambda$. ZPs of the kinoform type are convenient to attain the highest efficiency at a broad spectrum; moreover, in this Letter we neglect spurious light originated from different orders of diffraction. Illuminated by a point source (PS), the DOE is conveniently placed at a_1 in front of ZP_1. We point out that axial distances are oriented; specifically $a_1 > 0$ in Fig. 1, but a negative value would be considered if the DOE is virtually imaged at the rear of ZP_1 by means of a relay lens system (RLS) as given ahead. After diffracted light traverses ZP_1, a magnified replica of the DOE transmittance is observed at a_1' from the lens, evaluated from the lens formula $a_1^{-1}+a_1'^{-1}=f_1^{-1}$, where the lateral magnification is $M_1=-a_1'/a_1$. In this Letter lens aperturing is omitted. This image wave impinges over ZP_2 after propagating a distance $a_2=-a_1'+d$. In the image space, a new replica may be found at a distance a_2' from ZP_2, again computed by the lens formula $a_2^{-1}+a_2'^{-1}=f_2^{-1}$ and now affected by a lateral magnification $M=M_1M_2$ being $M_2=-a_2'/a_2$. In principle, a controllable dependence of M upon the wavelength may be achieved as a result of the dispersive character of f_n. Finally, if a plane wavefront of the output diffracted field results in convenience, the lens formula,

$$\frac{1}{R+a_1}+\frac{1}{d-f_2}=\frac{1}{f_1}, \tag{1}$$

provides the required radius of curvature R of the incident wavefront illuminating the DOE.

For simplicity, let us first assume the DOE has a phase-only transmittance $\exp(ik\mathbf{qr})$ exciting a single transverse frequency $k_0\mathbf{q}_0=k\mathbf{q}$ (subindex 0 points at λ_0). In the ZP-doublet image plane, the magnified wave field $\propto\exp(ik\mathbf{qr}/M)$ holds a spatial frequency $k\mathbf{q}/M$. This field represents a tilted plane wave, where angular deviation θ with respect to the z axis is evaluated from the equation $q/M=\sin\theta$, with q be-

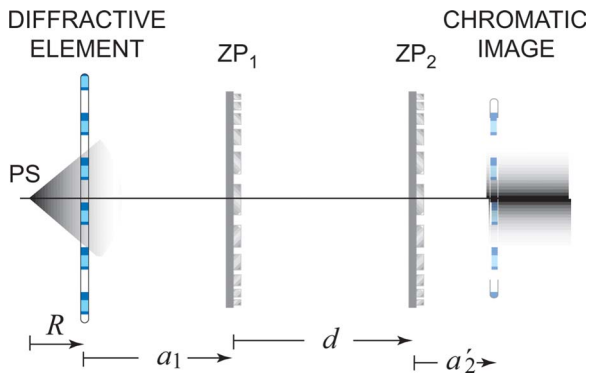

Fig. 1. (Color online) Schematic of dispersive ZP doublet.

0146-9592/08/151753-3/$15.00

ing the modulus of **q**. In the paraxial regime $\sin\theta \approx \theta$ leading to an output of cubic angular deviation

$$\theta = \theta_1\frac{\lambda}{\lambda_0} + \theta_2\left(\frac{\lambda}{\lambda_0}\right)^2 + \theta_3\left(\frac{\lambda}{\lambda_0}\right)^3, \tag{2}$$

where $\theta_1 = q_0$, $(\theta_2, \theta_3) = (\mu, \nu)\theta_1$, and

$$\mu = -\frac{a_1(Z_1+Z_2)}{Z_1Z_2} - \frac{d}{Z_2}, \tag{3a}$$

$$\nu = \frac{a_1 d}{Z_1 Z_2}. \tag{3b}$$

In the short-wavelength regime $\lambda \ll \lambda_0$, ZPs become zero-power ($f_n^{-1} \to 0$) lenses, and, as expected, angular deviation is dominated by the term $\theta_1 > 0$. However, strong deviations from this linear dependence upon wavelength may be found in the vicinity of λ_0. In particular $\theta_0 = \theta_1(1+\mu+\nu)$ may be negative, where an inversion about the z axis would be considered. We point out that ZP singlets may be investigated at $d = 0$, for which ν vanishes; in this case $\theta_3 = 0$ and, consequently, angular deviation is represented by a parabola [6].

Dispersion curves may be tailored by modifying geometric parameters of the optical system: DOE position (a_1), coupling distance (d), and ZPs focal distances (Z_n). In the vicinity of λ_0, normal DIAD is observed if $\dot{\theta}_0 > 0$ and anomalous DIAD is observed if $\dot{\theta}_0 < 0$, where the single dot represents a first derivative ∂_λ. When $\dot{\theta}_0 = 0$, leading to

$$1 + 2\mu + 3\nu = 0, \tag{4}$$

λ_0 represents a stationary point; thus, dispersion curves provide an achromatic response around λ_0. In Fig. 2 we show some dispersion curves for different values of the parameters μ and ν satisfying Eq. (4). We point out that these sorts of solutions are independent upon q so that the achromatic condition is satisfied simultaneously for every component of the angular spectrum. Finally, for a diffractive singlet ($d = 0$) of optical power $Z^{-1} = Z_1^{-1} + Z_2^{-1}$ (at λ_0) we encounter the solution $a_1 = Z/2$ given elsewhere [6,7].

In the anomalous regime, the curve changes from being concave downward having a maximum to concave upward containing a minimum (see curve D in Fig. 2). Therefore, a couple of wavelengths λ_- ($<\lambda_0$) and λ_+ ($>\lambda_0$) are found satisfying $\theta(\lambda_\pm) = \theta_0$. This apochromatic behavior allows ultraflattened dispersion curves in broadbands around λ_0; the lower $|\dot{\theta}_0|$ the flatter the curve. Furthermore, θ has an inflection point between $\lambda_\pm$, which may coincide at λ_0 if $\ddot{\theta}_0 = 0$, giving

$$\mu + 3\nu = 0. \tag{5}$$

Dispersion curves corresponding to solutions of Eq. (5) are shown in Fig. 2. If additionally $\dot{\theta}_0 \to 0$, giving $\mu = -1$ and $\nu = 1/3$ from Eqs. (4) and (5), a saddle point is found at λ_0 (see curve A in Fig. 2); hereupon, this solution is analyzed in detail.

First we encounter $\theta_0 = \theta_1/3$ so that apochromaticity of the output wave field is accompanied with a decrease of spatial frequencies. From Eqs. (3a) and (3b) we infer that ZPs and DOE may be positioned following

$$\left(\frac{a_1}{Z_1}\right)_\pm = \frac{1 \pm \sqrt{-\frac{4}{3}\left(\frac{Z_1}{Z_2}+\frac{1}{4}\right)}}{2\left(\frac{Z_1}{Z_2}+1\right)}, \tag{6}$$

$$\frac{d}{Z_2} = \frac{1}{3}\left(\frac{a_1}{Z_1}\right)^{-1}. \tag{7}$$

As a consequence, axial distances a_1 and d depend exclusively on focal distances Z_n. Equations (6) and (7) are plotted in Fig. 3. Real values are found if $Z_1/Z_2 \leqslant -1/4$, yielding air-spaced convergent–divergent pairs. In this case, axial distances a_1 and d have opposite signs. Since d is necessarily positive, we find that $a_1 < 0$; as a consequence, an RLS should be inserted between the diffractive element and ZP_1 to create a virtual DOE behind.

Of particular interest is the case of $Z_1 = -Z_2$, where $(a_1/Z_1)_- \to 1/3$ and $d = Z_2$; considering $(a_1/Z_1)_+$ leads trivially to the attachment of the ZPs ($d = 0$) and,

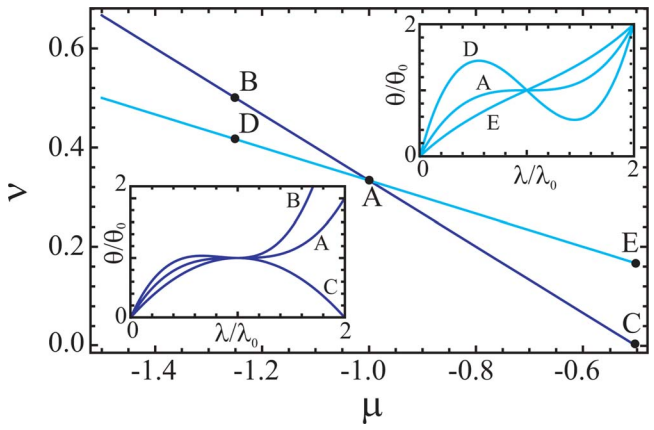

Fig. 2. (Color online) Dispersion curves (insets) with a stationary point (A, B, and C in black) and an inflection point (A, D, and E in gray) at λ_0.

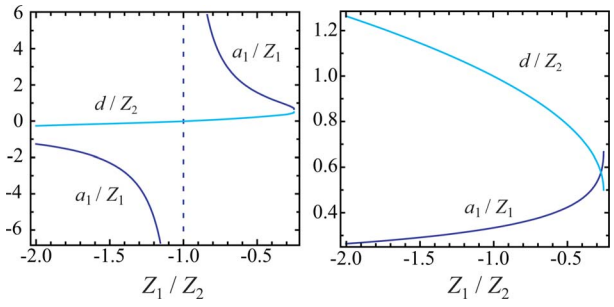

Fig. 3. (Color online) Plot of $(a_1/Z_1)_+$ (left) and $(a_1/Z_1)_-$ (right) given in Eq. (6) for different values of Z_n. Also (d/Z_2) of Eq. (7) is shown in the plots.

therefore, is rejected. Its relevance is better understood by analyzing the parameter

$$\frac{a_2'}{Z_2} = \frac{\lambda_0(\lambda - 2\lambda_0)}{\lambda^2 - 3\lambda\lambda_0 + 3\lambda_0^2}. \quad (8)$$

The DOE is imaged at a distance $a_2' = -Z_2$ (at λ_0) from ZP_2 in such a way that $\dot{a}_2'$ vanishes at λ_0. As a consequence, longitudinal chromatic aberration is compensated. We point out that a virtual image is formed since $a_2' < 0$ for a broadband around λ_0; however, an RLS may be placed behind to collect the wave field in a given (real) plane. Finally, $\ddot{a}_2' = 2Z2/\lambda_0^2 > 0$ at λ_0; in fact, this is an invariant for every apochromatic solution of Eqs. (6) and (7) and not only when $Z_1 = -Z_2$. We may conclude that a residual longitudinal chromatic aberration associated with the location of the imaged pattern remains unavoidable.

The proposed apochromatic arrangement is depicted in Fig. 4. A plane-wave source of time spectrum S is at the input plane. Following [7] we benefit from RLSs each made of two nondispersive refractive lenses of focal distance f and separated $2f$. They demonstrate three-dimensional shift-invariant imaging [8] with unit magnification and off-axis inversion. The RLS entrance plane is at f in front of the first lens, and the exit plane is at f behind the second lens. First, a so-called illuminating system is designed to transform the incident plane wavefront into the necessary spherical wavefront at the DOE plane. It consists of an RLS (with subindex 1 in Fig. 4) and a pair of ZPs of focal lengths $\pm Z_2$; the divergent ZP is located at d from RLS_1 entrance plane, and the convergent ZP is placed at its exit plane. At $-a_1 = Z_2/3$ beyond, where the DOE would be placed, the wavefront yields a radius of curvature

$$\frac{R}{Z_2} = \frac{\lambda^2 - 3\lambda\lambda_0 + 3\lambda_0^2}{3\lambda^2}, \quad (9)$$

as also required from Eq. (1).

Subsequent to suited illumination, the wave field diffracted by the DOE is chromatically corrected by means of a new ZP doublet. Before, RLS_2 virtually projects the diffracted wave field behind ZP_1 (of focal distance $-Z_2$) at $-a_1$. After traversing the compensating ZP doublet, the corrected pattern is imaged at a plane coinciding with the ZP_1 plane; thus, an ultimate unitary projection may be required. In this case, RLS_3 generates a tuned pulsed field at its exit plane (also output plane in Fig. 4). Importantly, the RLS_m entrance plane ($m = \{2,3\}$) matches at the RLS_{m-1} exit plane.

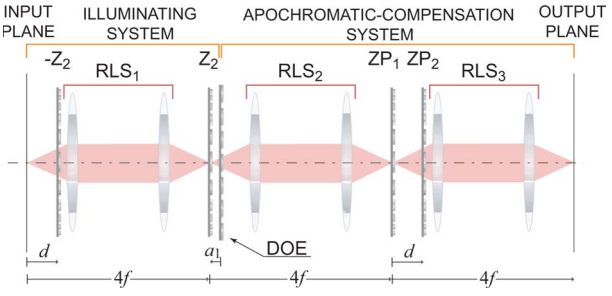

Fig. 4. (Color online) Schematic of arrangement.

In general DOE transmittance $T(\mathbf{r})$ may be represented as $\int A(\mathbf{q})\exp(ik\mathbf{qr})\mathrm{d}^2\mathbf{q}$, where A stands for the angular spectrum of the diffracted field under homogeneous illumination. Assuming hard-edge diffraction and, in general, any sort of wave modulation remaining T invariant upon k, A magnifies in direct proportion to k^{-1}. In the framework of the Fresnel–Kirchhoff diffraction formulation, the wave field at z from the output plane of coupled illumination-compensation systems yields an angular-spectrum representation

$$\Phi(\mathbf{r},z) = \int \tilde{A}(\mathbf{q})\exp(ik\mathbf{qr})\exp(ikmz)\mathrm{d}^2\mathbf{q}, \quad (10)$$

where $m = 1 - q^2/2$. Output angular spectrum

$$\tilde{A}(\mathbf{q}) = -SM^2A(M\mathbf{q})\exp[ik(Z_2 + a_2')q^2/2], \quad (11)$$

also modified by a quadratic phase term, manifests a magnification proportional to $(Mk)^{-1}$. Apochromatic correction guarantees that ∂_λ and ∂_λ^2 of Mk vanishes at λ_0. Unfortunately $\ddot{a}_2' \neq 0$ induces group-velocity dispersion (GVD) and, therefore, pulse stretching of transform-limited inputs S. In fact, GVD is also induced by material dispersion of lenses and ZPs.

In conclusion, we propose a novel arrangement exploiting ZP doublets, leading to angular dispersion of diffracted wave fields with apochromatic behavior. Our analysis may be of relevance in the generation of controlled broadband pulses and DOE-based ultrafast beam shaping [7].

This research was funded by the Generalitat Valenciana under the project GV/2007/043.

References

1. O. E. Martínez, Opt. Commun. **59**, 229 (1986).
2. Z. L. Horváth, Z. Benko, A. P. Kovacs, H. A. Hazim, and Z. Bor, Opt. Eng. (Bellingham) **32**, 2491 (1993).
3. N. Sanner, N. Huot, E. Audouard, C. Larat, J.-P. Huignard, and B. Loiseaux, Opt. Lett. **30**, 1479 (2005).
4. J. Amako, K. Nagasaka, and N. Kazuhiro, Opt. Lett. **27**, 969 (2002).
5. G. Li, C. Zhou, and E. Dai, J. Opt. Soc. Am. A **22**, 767 (2005).
6. C. J. Zapata-Rodríguez and M. T. Caballero, Opt. Lett. **32**, 2472 (2007).
7. C. J. Zapata-Rodríguez and M. T. Caballero, Opt. Express **15**, 15308 (2007).
8. D. N. Sitter and W. T. Rhodes, Appl. Opt. **29**, 3789 (1990).